Developmental Biology **216,** 348–358 (1999)
Article ID dbio.1999.9468, available online at http://www.idealibrary.com on IDEAL®

Suppression in *Urechis caupo*

Meredith C. Gould and José Luis Stephano

Facultad de Ciencias, Universidad Autónoma de Baja California, A.P. 2921, Ensenada 22800, B.C., Mexico

Although MAP kinase is an important regulatory enzyme in many somatic cells, almost nothing is known about its functions during meiosis, except in frog and mouse oocytes. We investigated MAPK activation and function in oocytes of the marine worm *Urechis caupo* that are fertilized at meiotic prophase. Activity was first detected at 4–6 min after fertilization in immunoblots with anti-active MAPK, prior to germinal vesicle breakdown (GVBD). MAPK activation did not require new protein synthesis and was dependent on the increases in both intracellular pH and intracellular Ca^{2+} that normally occur during activation. When MAPK activation was inhibited with PD98059 or U0126, GVBD still occurred, but meiosis was abnormal and there was a dramatic premature enlargement of sperm asters, which normally do not appear until second polar body formation. Failure of polar body formation and premature sperm aster enlargement also occurred when MAPK activation was inhibited by an entirely different treatment which involved lowering the pH of external seawater to interrupt the normal cytoplasmic pH increase. Thus, in *Urechis,* active MAPK appears to be required for (1) normal meiotic divisions and (2) suppressing the paternal centrosome until after the egg completes meiosis, a general phenomenon whose mechanism has been unknown.

Key Words: **meiosis; MAP kinase; sperm centrosome; germinal vesicle breakdown; PD98059; U0126; intracellular pH; intracellular Ca^{2+}.**

INTRODUCTION

Fully grown animal oocytes are arrested in meiotic prophase. In many species meiosis is reinitiated during ovulation and then the oocytes either complete meiosis prior to fertilization (e.g., sea urchins) or proceed to metaphase I (e.g., many bivalve molluscs, the annelid *Chaetopterus*) or II (e.g., vertebrates) where they arrest again until fertilization (Wilson, 1928; Austin, 1965). In other species (e.g., *Spisula* and *Urechis*) prophase oocytes are fertilized (Allen, 1953; Newby, 1932). When fertilization occurs during meiosis, the sperm nucleus waits in the egg periphery until both meiotic divisions are completed and then migrates inward to join the haploid egg nucleus (Wilson, 1928). Whether meiosis reinitiation begins before or at fertilization, it is accompanied by MAP kinase activation in all species studied to date. Multiple roles for the active enzyme have been identified in *Xenopus* oocytes: it is required for activation of the universal M-phase promoting factor leading to dispersion of the prophase nuclear envelope (germinal vesicle breakdown, GVBD) and is one, but not the only, factor required for avoiding a return to interphase between the first and second meiotic divisions and for arresting the oocytes at meiotic metaphase II prior to fertilization (e.g., Furuno *et al.*, 1994; Roy *et al.*, 1996; Sagata, 1997). In mouse oocytes, MAP kinase (MAPK) is not activated until after GVBD (Gavin *et al.*, 1994; Verlhac *et al.*, 1994), but is implicated in normal meiosis since inactivation of mos, a MAPK kinase kinase, inhibits or delays polar body formation, and some oocytes reform pronuclei instead of arresting at metaphase II (Sagata, 1997).

Little is known about MAPK function in invertebrate meiosis. In starfish oocytes (which complete meiosis upon hormonal stimulation but can be fertilized at any stage following GVBD; Miyazaki and Hirai, 1979) MAPK is activated after GVBD and in some species (Tachibana *et al.*, 1997; Sadler and Ruderman, 1998), but not all (Fisher *et al.*, 1998), is implicated in suppressing DNA replication in the female haploid pronucleus prior to fertilization. In *Spisula* and *Chaetopterus* oocytes, MAPK activation occurs before GVBD (Shibuya *et al.*, 1992; Eckberg, 1997), but its functions have not been clarified, except that it is not necessary for GVBD in *Chaetoperus* (Eckberg, 1997). Therefore, it is clear that more data are required to identify functions of

0012-1606/99 $30.00

MAPK during meiosis in different species and determine whether there are common targets. We investigated MAPK activation in *Urechis* oocytes, an especially favorable material for studying meiosis, fertilization, and parthenogenesis (Gould and Stephano, 1996) and report interesting new findings on the functions and mechanism of activation of this important kinase during meiosis reinitiation.

MATERIALS AND METHODS

Animals and Gametes

Adult worms were maintained at 15–16°C in a natural seawater aquarium with biological filter, and gametes were obtained as described previously (Gould, 1967). Oocytes were washed and stored in filtered (0.45 μm) natural seawater (SW) at 16°C and sperm were stored "dry" at 4°C.

Solutions and Reagents

Unless otherwise noted, filtered natural SW was buffered to pH 8 (the normal pH of SW) or pH 7 with 10 mM Tris–HCl. Synthetic sperm peptide P23 (Gould and Stephano, 1991) was used at 400 μg/ml in SW. For experiments in which oocytes were transferred to pH 7 after fertilization or activation with P23 at pH 8, buffer was omitted from the pH 8 SW. Emetine (Sigma; 10 mM stock solution in ethanol) was used at a final concentration of 100 μM. PD98059 (NE Biolabs) was diluted 1:1000 (final concentrations of 10, 50, and 100 μM) from stock solutions in anhydrous DMSO (Aldrich Chemical Co.). U0126 (Promega) was dissolved in DMSO and diluted 1:1000 or 1:2000 (final concentrations 50–0.04 μM).

Detection of Active MAP Kinase by Immunoblotting

Samples of oocyte suspensions (5% v/v) were centrifuged and pellets (5 μl; ~3500 oocytes) were resuspended in 5 μl 2× phosphatase + protease inhibitors (in mM: 100 β-glycerophosphate, 4 NaF, 2 Na_3VO_4, 2 PMSF, 40 EGTA, pH 7; leupeptin, pepstatin, aprotinin, 6.7 μg/ml each; Sigma) and then 25 μl 2× Laemmli (1970) sample buffer containing 3.6% SDS was added with rapid mixing. Samples dissolved completely at room temperature and were not boiled. Ten microliters (~1000 eggs, equivalent to about 50 μg TCA-insoluble protein; Miller and Epel, 1973) was loaded per well of SDS gels containing 10% acrylamide (Laemmli, 1970). Following electrophoresis, Coomassie blue staining showed uniform intensities in samples from different stages (not shown). Electrotransfer was to PVDF membranes (Applied Biosystems) and active MAPK was detected with affinity-purified polyclonal (Figs. 1A,1 C, and 2B, Promega; Fig. 2A, NE Biolabs) or monoclonal (Figs. 1B, 2C, and 6; NE Biolabs) anti-active MAPK, followed by donkey anti-rabbit (Promega or Affinity Bioreagents) or anti-mouse (Affinity Bioreagents) IgG peroxidase conjugate and ECL+ (Amersham). The Promega antibody was made against a synthetic peptide corresponding to the region containing pTEpY from the p42/ERK2 enzyme. The NE Biolabs antibodies were against KLH-coupled synthetic peptides corresponding to residues including pTEpY of human p44 MAPK. Figures 2A and 2B show that these antibodies reacted with a single band from *Urechis* eggs. For positive and negative controls we used the phosphorylated and nonphosphorylated MAPK control proteins (42-kDa erk2) from NE Biolabs (see Fig. 6). In our gels the phosphorylated erk2 protein migrated at about 44 kDa, and the *Urechis* active MAPK migrated at about 48 kDa. (Prestained standard protein ladders were from Bio-Rad or Gibco BRL.) The exposed X-ray films (Biomax ML, Kodak) were scanned with Adobe Photoshop and then average pixel intensities in rectangles drawn around the bands were measured with NIH Image. Background intensities obtained from adjacent regions were subtracted.

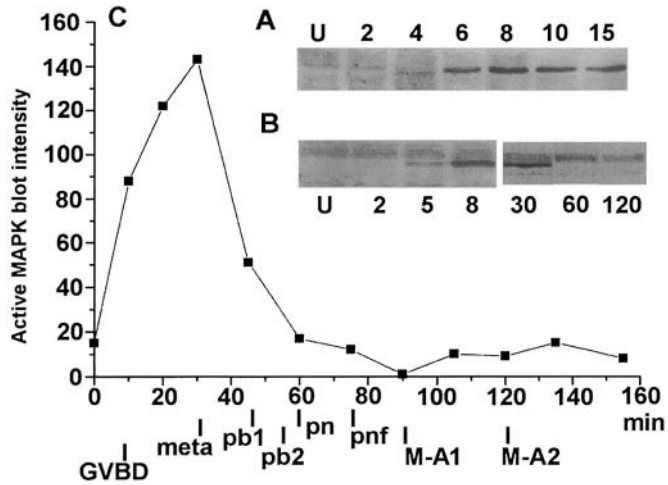

FIG. 1. Time course of MAPK activation during meiosis reinitiation. (A) Oocytes activated with sperm peptide P23 (400 μg/ml; Gould and Stephano, 1991). Sample times are in minutes; U, untreated. (B) MAPK activation 2, 5, 8, 30, 60, and 120 min after fertilization at pH 8 (1:20,000 sperm; U, unfertilized). Lanes U–8 and 30–120 are from two different experiments. GVBD occurred by 10 min in 100% of oocytes fertilized or exposed to P23 at pH 8. (C) MAPK activity during meiosis and mitosis of fertilized eggs. 0, unfertilized oocytes; GVBD occurred at 7 min, and at 20 min, chromosome congression was under way. Meta, metaphase I of meiosis (30 min); pb1, first polar body formation (45 min); pb2, second polar body formation (55 min). At 60 min (pn) chromatin is decondensing to form male and female pronuclei and by 75 min (pnf) the pronuclei have fused. M-A1, meta-anaphase of first cleavage; M-A2, meta-anaphase of second cleavage. Lanes 30, 60, and 120 in (B) are examples of data from this experiment.

Staining for Chromosomes and Sperm Pronuclei

Samples in SW were fixed for ≥30 min at room temperature by adding 1/3 vol of 4% formaldehyde in SW, washed 2–3× in SW, stained with bisbenzimide (H 33258, Calbiochem, 25 μg/ml in SW + 1mM Taps, pH 8), and viewed with the 60× oil immersion objective of an epifluorescence microscope (Olympus BH-2; see below). Photographs (T-Max or Ektachrome 100) were taken through a microscope adapter (Kalt Corporation, Santa Monica CA) on one of the oculars.

Immunofluorescent Staining with Anti-tubulin

Methods for anti-tubulin staining are described in Stephano and Gould (1995). Egg samples were harvested 10, 20, or 30 min after

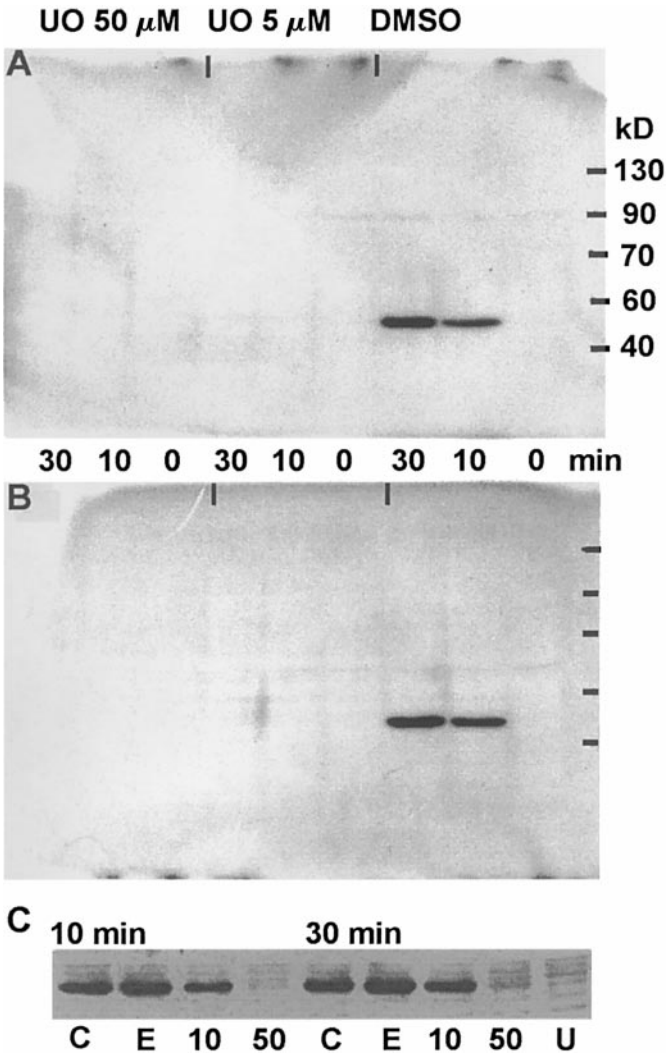

FIG. 2. Effects of inhibitors on MAPK activation. (A, B) Unfertilized oocytes were incubated in DMSO (0.05%) or 5 or 50 μM U0126 (0.05% DMSO) for 10 min, and then samples were taken (0) and the oocytes were fertilized 5 min later in the same solution (1:20,000 sperm dilution). Additional samples were taken at 10 and 30 min after fertilization. Both blots were incubated with polyclonal antibodies against active MAPK: A, NE Biolabs; B, Promega (see Materials and Methods). (C) Effects of emetine (E; 100 μM) and PD98059 (10 and 50 μM) at 10 and 30 min after fertilization. Both drugs were added 5 min before fertilization. C, control fertilized; U, unfertilized. MAPK activation was partially inhibited with 10 μM PD98059 and completely inhibited with 50 μM. Eggs in emetine form only one polar body and then arrest (also see Gould, 1968).

insemination with sperm diluted 1:1000–1:5000 (v/v) and washed 2× with OCa-SW (484 mM NaCl, 10 mM KCl, 27 mM $MgCl_2$, 29 mM $MgSO_4$, 2.4 mM $NaHCO_3$, pH 7) + 5 mM EGTA and then resuspended in 3 ml 0.75 M glucose + 5 mM EGTA, pH 7, to remove the vitelline coats. Three milliliters of OCa-SW + EGTA was then gently added, and following a brief centrifugation, the loose pellet was resuspended in extraction buffer [10 mM EGTA, 55 mM $MgCl_2$, 25% glycerol, 1% Nonidet P-40 (Pierce Chemical), 25 mM pipes, pH 6.8; Oka *et al.*, 1990]. The total time between addition of glucose–EGTA and resuspension in extraction buffer was about 2 min. Following 1–2 min in extraction buffer, drops of eggs were placed on polylysine- (1 mg/ml) coated slides and allowed to adhere for about 5 min before they were fixed by flooding repeatedly with cold (−20°C) methanol for 5–10 min. Following rehydration in dilution buffer (140 mm NaCl, 10 mm Tris–HCl, pH 6.8; Oka *et al.*,1990) the preparations were exposed to antibodies in dilution buffer containing 10% goat serum (Sigma). Monoclonal anti-β-tubulin and fluorescein-conjugated sheep anti-mouse IgG were from Boehringer-Mannheim. Antibody incubations were for 0.5 h each at 37°C, followed by three 15-min washes with dilution buffer at room temperature. Preparations stained with bisbenzimide (25 μg/ml in 0.1 M phosphate buffer, pH 7.2) were first rinsed with phosphate buffer (bisbenzimide precipitates in dilution buffer). Slides were drained and mounted with 0.24% *n*-propyl gallate (Sigma) in 90% glycerol (Giloh and Sadat, 1982). Tubulin staining was examined by confocal scanning laser microscopy (Bio-Rad MRC 600; excitation 488 nm) with a 60× oil immersion objective (SPlanApo, N.A. 1.4), and then bisbenzimide staining was recorded by switching to normal epifluorescence (excitation 350 nm) on the same microscope (Olympus BH-2) and photographing images through the ocular as described above.

RESULTS

MAP Kinase Activation during Meiosis Reinitiation

Active MAP kinase was first detected 4–6 min after fertilization or activation with the sperm acrosomal peptide P23 (VAKKPK; Gould and Stephano, 1991) just prior to GVBD at 7 min (Figs. 1A and 1B). Activity continued to increase, reached a peak during metaphase I, declined gradually during polar body formation, and returned to unfertilized oocyte levels during pronuclear formation (Figs. 1B and 1C). Similar increases during meiosis reinitiation were observed in six of six experiments with fertilization and three of three with sperm peptide and the decline after polar body formation was observed in all four experiments (two with sperm and two with P23) where this was followed. Significant increases were not detected during the first two mitotic cleavages in fertilized eggs (Figs. 1B and 1C).

The increase in active MAPK was eliminated in the presence of two different drugs that are reported to be highly specific inhibitors (see Discussion) of the activation of MEK, the kinase that activates MAP kinase. U0126 (Favata *et al.*, 1998; DeSilva *et al.*, 1998) was effective at 5 μM (Figs. 2A and 2B) and PD98059 (Dudley *et al.*, 1995; Alessi *et al.*, 1995; Cross and Smythe, 1998) was effective at 50 μM (Fig. 2C).

MAPK activation still occurred when protein synthesis was inhibited by emetine (Fig. 2C, lanes E). This result shows that the components of the MAPK signaling cascade are already present in unfertilized oocytes, but one or more

of the upstream activators (e.g., MEK or MEK kinase) must be activated when meiosis is reinitiated.

Inhibition of MAP Kinase Activation Affects Polar Body Formation, but Not GVBD

To investigate whether meiosis reinitiation required MAP kinase activation, oocytes were fertilized in the presence of PD98059 and U0126. Germinal vesicle breakdown was not inhibited by 50 μM PD98059 (100% in two experiments each with $n > 50$) and occurred at the normal time. Even with 100 μM PD98059 100% of oocytes underwent GVBD (two experiments each with $n \geq 50$). GVBD also occurred at the normal time (7 min) in four of four experiments with 50 μM U0126.

However, in the PD98059-treated oocytes examined at 30 min after insemination, normal metaphase figures (Fig. 3A) were never observed. The maternal chromosomes appeared to condense normally, but chromosome congression was incomplete (Fig. 3B). Polar bodies were never observed in five of five experiments with 50 μM PD98059 (0/309 oocytes scored at 1–5 h after fertilization). Instead, the oocytes tended to remain arrested with scattered condensed chromosomes as in Fig. 3B for over 1 h. After this time chromosomes frequently began to decondense and by 4 h the eggs were typically filled with various mitotic figures and chromatin masses in interphase (not shown).

U0126-treated oocytes also failed to complete meiosis. Normal first polar body formation in DMSO-treated control oocytes is illustrated in Fig. 3C: the chromatin in the polar body (pb) is highly compacted and the chromosomes in the egg remain condensed prior to second polar body formation. U0126-treated oocytes reached metaphase I at the normal time (30 min), but then they formed an abnormally large first polar body and proceeded directly to the pronuclear stage without second polar body formation. Figure 3D shows a U0126-treated egg: polar body formation is slightly delayed and the chromosomes are not as compacted as in the control (Fig. 3C). Right after first polar body formation, the maternal chromosomes, sperm pronuclei, and even the chromatin in the polar body begin to decondense (Fig. 3E). Typical polar bodies in control and U0126-treated eggs are shown in Figs. 3F and 3G. Normal-sized first polar bodies were never observed in six of six experiments with 5 and 50 μM UO126 (0/260 and 0/200 eggs at the two concentrations, respectively) and second polar bodies never formed. The same effects were seen when eggs were activated with sperm peptide (P23) instead of sperm. The threshold concentration of U0126 required to produce these effects (enlarged first polar body and advancement to the pronuclear stage without second polar body formation) was 0.2 μM (100%; $n = 50$); with 0.04 μM, second polar body formation was normal (100%; $n = 50$).

Eggs fertilized in U0126 divided mitotically, although cleavage was generally abnormal. Cytokinesis did not occur in PD98059-inhibited eggs, although the presence of multiple interphase nuclei and mitotic figures indicated that the chromosomes were cycling.

In conclusion, the above results show that MAP kinase activity increases dramatically after fertilization or activation with sperm peptide and is required for normal polar body formation, but not for GVBD and chromosome condensation.

PD98059- and U0126-Inhibited Eggs Contain Prematurely Enlarged Sperm Asters

The failure of egg chromosomes to line up normally on a metaphase plate and undergo meiotic divisions when MAP kinase activation was inhibited with PD98059 suggested that aster and/or spindle formation were affected. This possibility was investigated by immunocytochemistry with anti-tubulin antibodies. The results show that maternal asters developed and separated in the presence of PD98059, but normal spindles did not form (20/22 eggs; Figs. 4A and 4B). Even when an apparently normal spindle did form not all the chromosomes were included (Figs. 4C and 4D). These results suggest that the inhibitor might affect the normal interactions between kinetochores and microtubules that collect the chromosomes and form the spindle.

Another dramatic effect of MAPK inhibition was revealed by these experiments. During normal fertilization aster formation does not begin until second polar body formation (Stephano and Gould, 1995). However, in the presence of PD98059, large sperm asters were visible as early as 10 min after insemination (not shown) and were present in 22/22 eggs scored at 30 min; Figs. 4A and 4C). Furthermore, these sperm asters tended to be clustered around the area where the female asters and chromosomes were located. Frequently the sperm asters were paired (Figs. 4A and 4C) suggesting that the centriole pair introduced by the sperm (Luykx, 1991) may have separated or duplicated, although these possibilities would require confirmation by electron microscopy.

When MAPK activation was inhibited, the sperm pronuclei also tended to migrate toward the center of the egg (Figs. 4B, 4D, and 4F) whereas normally the sperm pronuclei remain near the periphery of the egg and do not migrate into the center until after polar body formation (compare Figs. 4E and 4F; also see Stephano and Gould, 1995).

Premature sperm aster development also occurred in the U0126-inhibited eggs and these asters and sperm pronuclei also tended to migrate into the vicinity of the egg asters (Fig. 5A, 15/15 eggs). Sperm asters were not present in DMSO-treated control eggs from the same experiment (Fig. 5B, 14/14 eggs; also see Stephano and Gould, 1995). Typically the male pronucleus appeared stretched as if it were being dragged by its aster (Figs. 3D and 5A). Stretched sperm chromatin was also common at 30 min after fertilization in eggs exposed to 0.2 μM U0126 (not shown) indicating that premature sperm asters were present even at this low concentration of inhibitor. Stretched sperm pronuclei were also present in PD98059-treated eggs (Fig. 3B inset). In

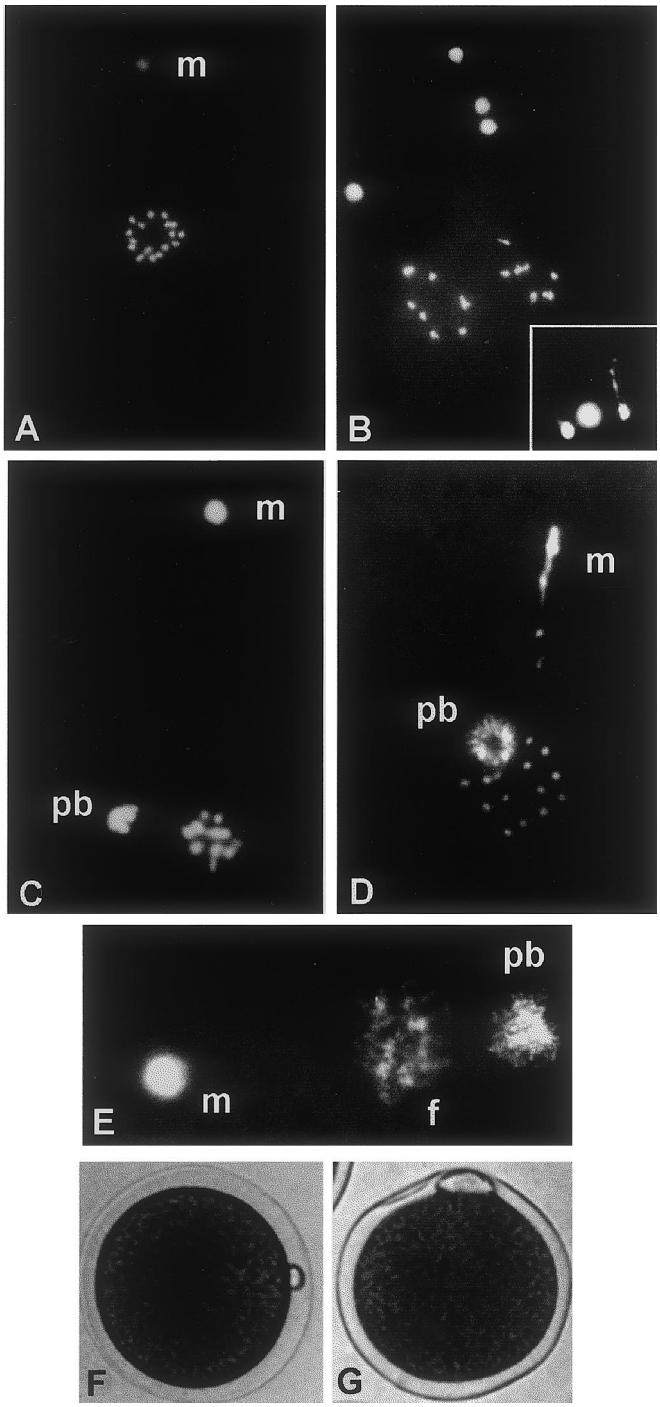

FIG. 3. Effects of PD98059 and U0126 on chromosome behavior during meiosis reinitiation. Chromatin is stained with bisbenzimide. (A) Control fertilized egg at 30 min after insemination (1:25,000 sperm dilution) showing the 17 tetravalent chromosomes in metaphase of the first meiotic division and the sperm pronucleus (m). (B) PD98059-treated eggs at 30 min after insemination (1:5000 sperm) showing incomplete chromosome congression. Four sperm pronuclei are visible. (See text for discussion of the increased polyspermy in PD98059.) By 1 h sperm pronuclei are frequently stretched as if they were migrating (inset). (C) Control DMSO-treated egg fixed at 45 min after fertilization. Chromatin in the first polar body (pb) is highly compacted and the adjacent condensed chromosomes are in metaphase II. The sperm pronucleus (m) is above. (D) Oocyte pretreated for 10 min in 50 μM U0126 and then fertilized in the presence of the inhibitor and fixed at the same time as the egg in (C). Chromosomes are less aggregated than normal in the forming polar body (pb) as well as in the egg, and the sperm pronucleus (m) is stretched as if it were being dragged toward the egg chromosomes. (E) A slightly more advanced egg from the same sample as (D). Following polar body formation, chromatin rapidly decondenses in the polar body (pb) oocyte chromosomes (f) and sperm pronucleus (m; slightly out of focus). (F) Living control (DMSO) egg with first polar body photographed at 47 min after fertilization. (G) Living U0126-treated egg (50 μM) with typical enlarged polar body 58 min after fertilization. In this sample, normal first polar bodies were 15–17 μm in diameter along the long axis (15.8 $\pm$ 0.8, mean $\pm$ SD, $n = 11$) and the polar bodies in U0126-treated eggs ranged from 22 to 75 μm (33.8 $\pm$ 11.6, $n = 17$; $P << 0.01$). Eggs (120 μm diameter) in (F) and (G) were photographed without coverslips.

control eggs, stretched sperm chromatin was never observed before second polar body formation (e.g., Fig. 3C; also see Stephano and Gould, 1995).

A side effect of PD98059 (50 μM) treatment was increased susceptibility to polyspermy. In two experiments employing high sperm concentrations (1:5000 v/v dilution) the average number of sperm entries per egg was 2.5 (range 2–8) and 1.5 (1–-5) in the control samples and 6.7 (4–11) and 4.8 (2–11) in the respective experimental samples. On the other hand, U0126 had very little effect on polyspermy. For example, in an experiment with 1:5000 sperm dilution, the average number of sperm/egg was 1.58 (1–4) in control eggs (DMSO) and 1.83 (1–4) in experimental eggs (50 μM U126). At lower sperm concentrations (1:20,000) there was only a small difference between control eggs (1.23; 1–6) and those in 50 μM U0126 (1.74; 1–7) and essentially no difference with lower concentrations of U0126 (e.g., DMSO, 1.16, 1–3; 5 μM U0, 1.22, 1–4; 0.2 μM U0, 1.21, 1–5; 0.04 μM U0, 1.21, 1–3). The effect of PD98059 on the electrical polyspermy block will be the subject of a separate communication.

Inhibition of MAP Kinase Activation by a Different Treatment Also Permits GVBD, Inhibits Polar Body Formation, and Causes Premature Sperm Aster Enlargement

We noted a striking resemblance between the PD-inhibited oocytes and oocytes subjected to a very different treatment. When *Urechis* oocytes are transferred to pH 7 SW at about 2 min after insemination or activation with the sperm peptide P23, proton release stops (normal SW is pH 8) and the intracellular pH increase required for complete activation is interrupted (Stephano and Gould, 1997a). These oocytes undergo GVBD, chromosomes condense, and

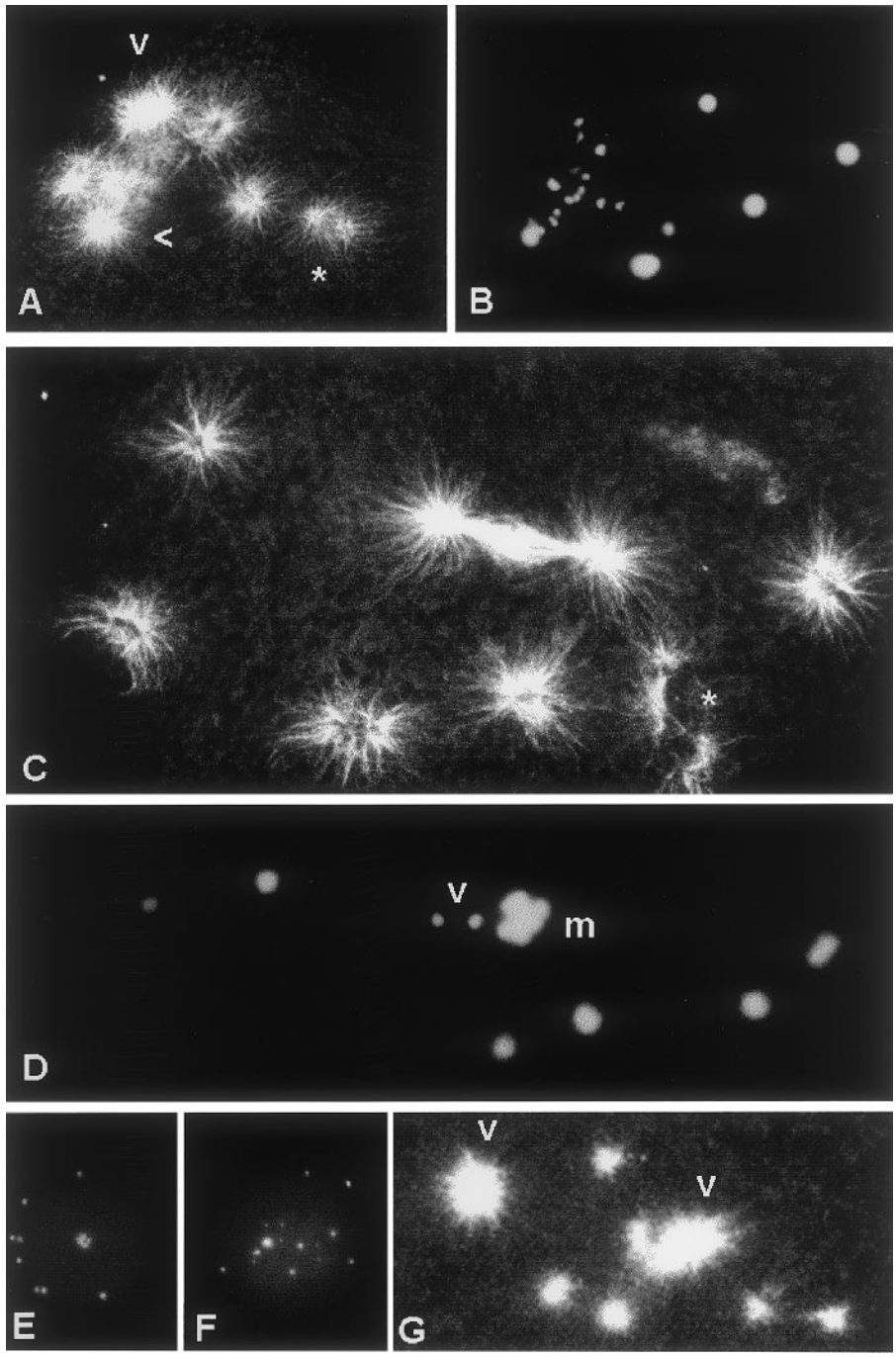

FIG. 4. Effects on aster development and chromosome behavior when MAPK activation is inhibited with PD98059 or a pH shift. (A) PD98059- (50 μM) treated egg 30 min after insemination. Six large sperm asters are present as well as the two maternal asters (arrows). One of the sperm asters is clearly double (*). (B) Bisbenzimide staining of the same egg showing the scattered egg chromosomes and sperm pronuclei (5 are visible; the sixth was out of focus below the chromosomes). In control oocytes all 17 tetravalent chromosomes are aligned on the metaphase plate (see Fig. 3A). (C) One of two cases in which a meiotic spindle formed; but bisbenzimide staining (D) reveals two unincorporated chromosomes (arrow) that were outside the metaphase cluster (m). Six sperm pronuclei (D) and six sperm asters (C) are present; one is double (*) and others give the impression they could have two centers. (E and F) Bisbenzimide-stained eggs 30 min after insemination (1:5000 sperm). Sperm pronuclei in control eggs (E; eight sperm) remain in the cortex until meiosis is completed; however, they tend to migrate inward prematurely in PD98059-treated eggs (F; also eight sperm). (G) Fertilized egg transferred to pH 7 SW at 2 min 10 s to prevent MAPK activation and fixed at 30m for anti-tubulin staining. Here also, egg asters (arrows) do not form a spindle and sperm asters enlarge prematurely (three pairs are present). Several confocal sections are superimposed in (C) and (G) to reveal all the sperm asters.

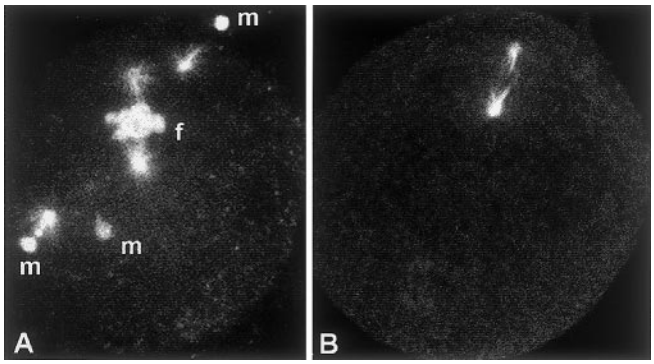

FIG. 5. (A) Premature sperm aster development in a U0126-treated (50 μM) egg 20 min after fertilization. A well-developed aster is associated with each sperm nucleus (m; the aster associated with the middle sperm nucleus is out of focus in this confocal image). Stretched sperm chromatin is clearly visible in two of the three pronuclei. f, maternal chromosomes. The excitation and emission spectra of bisbenzimide overlap sufficiently with those of fluorescein to permit simultaneous detection. (B) Typical control egg (DMSO-treated) 20 min after fertilization from the same experiment. No sperm asters are visible. (The egg was not stained with bisbenzimide.)

the maternal centrosome duplicates and forms asters, but chromosome congression, spindle formation, and polar body extrusion fail (Stephano and Gould, 1995).Therefore, we investigated MAPK activation in oocytes subjected to this treatment and found that it was undetectable (Fig. 6, lanes p). In the control oocytes exposed to P23 and maintained at pH 8, changes in MAPK activity were the same as in fertilized eggs: activity rose to a peak during first polar body formation and then declined (Fig. 6, unmarked lanes). Oocytes activated by P23 at pH 8 develop normally through second polar body formation and undergo repeated cycles of chromosome replication, but they fail to divide mitotically because the maternal centrosomes are inactivated during meiosis; Gould and Stephano, 1991; Stephano and Gould, 1995.)

Using the same treatment (transfer to pH 7) we were able to test the prediction that premature sperm aster enlargement should also occur in these eggs if MAPK is the suppresser of male centrosome activation before meiosis. Eggs were fertilized and then transferred to pH 7 SW at 2 min 10 s after insemination. The results are illustrated in Fig. 4G; enlarged sperm asters were present in 38/38 eggs examined 30 min later and they also occurred in pairs.

The results above reveal a new function for MAPK: repressing male centrosome activation until after meiosis. This could be important for preventing the sperm aster from interfering with meiosis. The decline in MAPK activity after polar body formation (Fig. 1C) could then be the signal for the sperm aster to enlarge and promote the migration of male and female pronuclei to fuse in the center of the egg. The 4- to 6-min delay between insemination and detectable MAP activity does not conflict with this hypothesis, since the sperm centrioles do not enter the egg cytoplasm until about 5 min after insemination (Tyler, 1965).

Increases in both Intracellular Ca^{2+} and Intracellular pH Are Required for MAP Kinase Activation

The absence of MAPK activation in eggs transferred to pH 7 provides an important clue to the mechanism of activation, indicating that intracellular alkalinization may be a requirement. Previous work has shown that increases in both intracellular pH and intracellular Ca^{2+} are necessary for GVBD and polar body formation in *Urechis* (Paul, 1975; Gould and Stephano, 1993; Stephano and Gould, 1997b). At fertilization or activation with P23, Ca_i rises rapidly to an initial peak within 16 s and then falls slightly and remains elevated through at least 10 min after fertilization (Stephano and Gould, 1997b). The pH_i increase begins later, about 20–30 s after insemination, reaches a plateau at about 3 min, and remains elevated through polar body formation (Gould and Stephano, 1993; Stephano and Gould, 1997a). When oocytes are inseminated in pH 7 SW, sperm enter and there is a normal prolonged Ca_i increase although pH_i does not rise and no activation occurs (Paul, 1975; Gould and Stephano, 1993; Stephano and Gould, 1997b); therefore, the Ca_i increase would also be normal when the pH of the external SW is changed to 7 at 2 min after fertilization or peptide addition. The converse, a large pH_i increase without a Ca_i increase, is produced by exposing unfertilized oocytes to NH_4Cl in the presence of Co^{2+} to block the Ca^{2+} channels (these oocytes do not activate; Stephano and Gould, 1997b. NH_4Cl alone causes both Ca_i and pH_i increases and the eggs activate and form polar bodies).

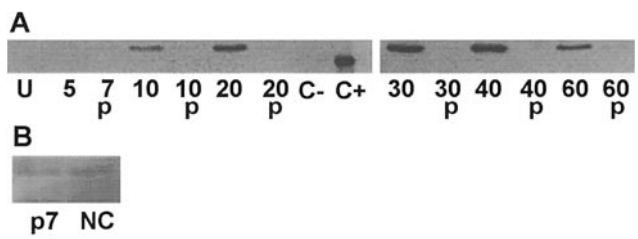

FIG. 6. (A) P23 was added to oocytes in pH 8 SW, and then some were resuspended in pH 7 SW at 2 min 10 s (p, partially activated; GVBD occurred in 70% of these oocytes, but none formed polar bodies, and 35% eventually began to cleave parthenogenetically; see Stephano and Gould, 1995, 1997) and the rest (no letter below the time) were left at pH 8 with P23 (first polar body formation began at 50 min) Samples were taken at the times (min) indicated. U, untreated; C− and C+ are negative and positive controls (nonphosphorylated and phosphorylated 42-kDa erk2 proteins; see Materials and Methods). (B) Active MAPK was not detected in oocytes fertilized in pH 7 SW (p7; 8 min after insemination) or exposed to 50 mM NH_4Cl + 20 mM $CoCl_2$ without sperm (NC; 8 min later). None of the oocytes underwent GVBD. These data are from the same immunoblot shown in Fig. 1B.

Using these treatments to produce the Ca_i and pH_i increases separately, we found that neither alone was sufficient to activate MAPK; both are required (Fig. 6B, p7 and NC). Fertilization at pH 7 was repeated once and treatment with $NH_4Cl + Co^{2+}$ was repeated three times with the same result. We are currently investigating how Ca^{2+} and pH act together to initiate MAPK activation in *Urechis* oocytes.

DISCUSSION

Our results show that meiosis reinitiation in *Urechis* eggs is accompanied by a dramatic temporary rise in active MAP kinase, beginning shortly before GVBD and lasting through polar body formation. Enzyme activation was stimulated both by sperm and by the sperm acrosomal peptide VAKKPK (P23), previously shown to induce eggs to undergo the same sequence of changes that normally follow fertilization (Gould and Stephano, 1991). MAPK activation required increases in both intracellular Ca^{2+} and intracellular pH, but no new protein synthesis. When MAPK activation was inhibited, meiosis was abnormal and sperm asters developed prematurely.

Sperm Asters

A striking effect of all three different treatments that inhibited MAPK activation after fertilization or activation with P23 was the activation of sperm centrosomes to form prominent asters well before the normal stage at second polar body formation. Two of the treatments employed drugs shown to be highly specific for inhibiting MEK, the kinase that activates MAPK. PD98059 (50 μM) was shown to be ineffective against a variety of other kinases both *in vivo* and *in vitro* by Alessi *et al.* (1995; other studies are reviewed in Cohen, 1997). U0126 was also tested with a variety of other kinases and shown to be specific for MEK and to be effective at lower concentrations than PD98059 (e.g., the IC_{50} against a constitutively active MEK *in vitro* was 0.07 μM for U0126 and 10 μM for PF98059, although 10 μM U0126 was required to completely inhibit ERK phosphorylation in cultured cells; Favata *et al.,* 1998). While Alessi *et al.* (1995) concluded that PD98059 inhibited MEK activation, Favata *et al.* (1998) showed that PD98059 could also inhibit previously activated MEK (see their article for a detailed comparison of the two inhibitors). Whether the two inhibitors share common binding sites is under investigation (Favata *et al.,* 1998). The third treatment that inhibited MAPK activation was just a simple pH shift (from 8 to 7) in the external seawater. As explained under Results, this interrupts proton efflux so the normal pH_i increase is not achieved. While this treatment does not necessarily inhibit only MAPK activation, it provides powerful correlative evidence since the effect on sperm asters was the same.

The sperm asters in the MAPK-inhibited eggs also appeared to be actively dragging their pronuclei through the egg cytoplasm, since stretched sperm chromatin was so commonly seen (e.g., Figs. 3B and 3D). Sperm pronuclei were also frequently observed clustered around the meiotic chromosomes (e.g., Figs. 4B, 4D, and 4F). Normally, sperm pronuclei tend to remain in the cortex of the egg until meiosis is completed and stretched sperm pronuclei (often connected to aster fibers) are not observed until sperm aster formation at the second meiotic division (Stephano and Gould, 1995).

Therefore, we conclude that our results identify a new role for MAPK during meiosis: suppressing the development of the sperm centrosome until after meiosis is completed. This delay in sperm centrosome activation is a "classic" observation in many species (e.g., Wilson, 1928, and references below), but to our knowledge our data provide the first evidence for a mechanism. This function for MAPK could explain some previously unexplained observations on the timing of CSF and MAPK inactivation after fertilization. In *Xenopus* oocytes, although mos (and therefore presumably active MAPK) is one of the components of CSF required to maintain the metaphase II arrest prior to fertilization, it (and CSF) is not inactivated until after second polar body formation (Watanabe *et al.,* 1991). Why CSF should remain active after it is no longer needed to maintain metaphase has had no functional explanation. Our results with *Urechis* suggest that active MAPK persists to suppress sperm aster formation until after meiosis is completed. In agreement with this hypothesis, sperm asters begin to grow at about the time of second polar body formation in *Xenopus* eggs (Stewart-Savage and Grey, 1982). Also, in an article by Guadagno and Ferrell (1998), there is a brief mention that sperm centrioles formed larger asters in *Xenopus* cytoplasmic extracts when MEK was immunodepleted or PD98059 was added. In mouse oocytes, MAPK is inactivated well after second polar body formation and the decline in activity is correlated with growth of asters in the cytoplasm (Verhlac *et al.,* 1994). Mice are unusual in that their centrosomes are apparently maternally inherited (Schatten *et al.,* 1986), so our hypothesis could be extended to include maternal mitotic asters (as well as the paternal centrosome?) in this case.

MAPK control of sperm aster development could also explain the interesting situation in starfish oocytes where fertilization causes MAPK inactivation, but the timing depends on the stage in meiosis when sperm are added. When oocytes are fertilized at second polar body formation or after meiosis is completed, enzyme inactivation begins rapidly (within 10 min), but when fertilization is at earlier stages, inactivation is delayed until just before second polar body formation (Picard *et al.,* 1996; Tachibana *et al.,* 1997). In agreement with our hypothesis, the major growth of the sperm aster is reported to begin after first or second polar body formation (e.g., Wilson and Mathews, 1895; Chambers and Chambers, 1949; Hirai *et al.,* 1981; Sluder *et al.,* 1989) although small sperm asters are detected soon after fertilization (Hirai *et al.,* 1981; Sluder *et al,* 1989). According to Hirai *et al.* (1981) these became "obscure" between the first and second meiotic divisions and then enlarged rapidly after

second polar body formation. These observations are consistent with our hypothesis.

Conflicting data were reported by Picard and Peaucellier (1998) whose preparations contained large sperm asters following insemination of prophase oocytes which were unaffected by microinjecting recombinant mos. These observations warrant reexamination since typically neither paternal nor maternal asters form until about the time of GVBD (*op. cit.* and Kato *et al.*, 1990).

The situation in *Spisula* oocytes is also consistent with our hypothesis. Here, MAPK is activated before GVBD and inactivated at about the time of second polar body formation (Shibuya *et al.*, 1992), when sperm asters are first detected by electron microscopy (Longo and Anderson, 1970) or anti α-tubulin immunocytochemistry (Kuriyama *et al.*, 1986). Using an antibody against γ-tubulin, Wu and Palazzo (1999) detected a small paternal aster before metaphase I that disappeared during meiosis I and then reappeared and grew after meta II.

It will be interesting to determine whether MAPK suppresses sperm aster formation in other species. It will also be important to identify the MAPK targets involved in suppressing sperm centrosome activation in *Urechis*. How aster formation by centrosomes is regulated in any cell type is not well understood (e.g., review by Zimmerman *et al.*, 1999) and *Urechis* provides favorable material to investigate this question.

Abnormal Meiosis

Meiosis was abnormal with all three treatments that inhibited MAPK activation. With PD98059 and the pH shift, the eggs failed to reach metaphase of the first meiotic division. Normal egg asters were formed and chromosomes condensed, but congression was incomplete and polar bodies never formed. On the other hand, eggs treated with U0126 did reach metaphase, but then formed an abnormal first polar body and quickly advanced to the pronuclear stage without forming the second polar body. It is not clear why the two inhibitors gave different results. Chromosomes in the PD98059- and pH shift-treated eggs also eventually decondensed, although more slowly (after 1–2 h; see Stephano and Gould, 1995, for a detailed description of events in eggs subjected to the pH shift). Thus, although details differed, all three treatments affected chromosome and spindle behavior.

How do these effects compare to those from other species? As mentioned in the Introduction, active MAPK is required for normal meiotic divisions in all species where this has been studied. In *Xenopus* oocytes, inhibition of MAPK at the time of GVBD with mos antisense oligonucleotides or anti-mos antibodies results in chromosome decondensation and DNA synthesis following first polar body formation (Furuno *et al.*, 1994; Roy *et al.*, 1996). In mos−/− knockout mice, first polar bodies usually form (although sometimes with delays and abnormal spindles), but then the oocytes fail to arrest normally in metaphase II and tend to reform pronuclei or even cleave (reviewed by Sagata, 1997). *Urechis* eggs inhibited with U0126 also formed pronuclei right after first polar body formation and proceeded to mitosis (we did not examine DNA synthesis directly, but it was obviously occurring since the DNA content in cleavage nuclei was maintained). In fact, the abnormally large first polar bodies in U0126-inhibited *Urechis* eggs look very much like those described by Choi *et al.* (1996; compare their Fig. 3 with our Fig. 3). In the mos−/− mice, the formation of the large polar bodies was correlated with failure of spindle migration to the cortex (Choi *et al.*, 1996). These effects in *Xenopus* and mouse resemble those produced by U0126 in *Urechis* eggs.

On the other hand, in another study with mouse oocytes, injection of anti-mos antibody produced a phenotype that was strikingly similar to that in the PD98059- and pH shift-treated *Urechis* eggs: chromosomes were scattered, spindles were abnormal, and no polar bodies formed (Zhao *et al.*, 1991). Why the effects of inhibiting MAPK activation were apparent at a slightly earlier stage in meiosis in these cases is not clear. In starfish oocytes inhibited with 50 μM PD98059, the effects were evident somewhat later: formation of both polar bodies apparently occurred, but the authors mention preliminary observations that the meiosis II spindle and chromosome segregation were abnormal (Sadler and Ruderman, 1998).

Therefore, while details differ, these studies implicate common targets for MAPK involved in regulating chromosome and spindle behavior during meiosis. Active MAPK has been localized on spindles, asters, and kinetochores in mitotic cells (Shapiro *et al.*, 1998; Zecevic *et al.*, 1998) and can phosphorylate microtubule-associated proteins (e.g., review by Gunderson and Cook, 1999).

pH and Ca^{2+} Requirements

Our results show that MAPK was not activated when eggs were fertilized in pH 7 seawater (Fig. 6B, p7), where the intracellular Ca^{2+} increase is normal (Stephano and Gould, 1997b) but no pH_i increase occurs (Gould and Stephano, 1993). MAPK was also not activated when eggs were activated with sperm peptide at pH 8, and then the pH of the external SW was adjusted to 7 about 2 min later (Fig. 6). Under these conditions, pH_i increases only slightly ($<$0.2 pH units) or returns to control values (the normal increase with P23 activation is 0.3–0.4 units; Stephano and Gould, 1997a), but the Ca_i increase would also be normal (Stephano and Gould, 1997b). A pH_i increase without a Ca_i increase is induced by exposure to NH_4Cl + Co^{2+} in the absence of sperm (Stephano and Gould, 1997), and under these conditions MAPK also failed to activate (Fig. 6B, NC). These results show that MAPK activation requires both Ca_i and pH_i increases.

To our knowledge, ionic requirements for MAPK activation during meiosis have not been studied in other species with the exception of *Spisula*. MAPK activation occurred in unfertilized oocyte lysates when the pH was raised from 6.8

to 7.2 (Walker *et al.*, 1996; Ca^{2+} was apparently not chelated) and activation in lysates at pH 7.4 required Ca^{2+} (Katsu *et al.*, 1999). (Increases in both Ca_i and pH_i occur at fertilization in intact oocytes; reviewed by Colas and Dubé, 1998.) How these ions control MAPK activation remains to be discovered.

ACKNOWLEDGMENTS

We thank Manuel Ornelas Orozco for laboratory assistance and Edward Salinas for collecting and shipping animals. This work was partially supported by the Consejo Nacional de Ciencia y Tecnología (3034 PN) and the Fondo para la Modernización de la Educación Superior.

Note added in proof. Recent experiments reveal that oyster sperm centrosomes are also activated prematurely when MAPK is inhibited with UO126 (Stephano and Gould, unpublished).

REFERENCES

Alessi, D. R., Cuenda, A., Cohen, P., Dudley, D. T., and Saltiel, A. R. (1995). PD 98059 is a specific inhibitor of the activation of mitogen-activated protein kinase *in vitro* and *in vivo. J. Biol. Chem*. **270,** 27489–27494.

Allen, R. D. (1953). Fertilization and artificial activation in the egg of the surf clam *Spisula solidissima. Biol. Bull.* **105,** 213–239.

Austin, C. R. (1965), "Fertilization." Prentice–Hall, Englewood Cliffs, NJ.

Chambers, R., and Chambers, E. L. (1949). Nuclear and cytoplasmatic interrelations in the fertilization of the *Asterias* egg. *Biol. Bull.* **96,** 270–282.

Choi, T., Fukasawa, K., Zhou, R., Tessarollo, L., Borror, K., Resau, J., and Vande Woude, G. F. (1996). The Mos/mitogen-activated protein kinase (MAPK) pathway regulates the size and degradation of the first polar body in maturing mouse oocytes. *Proc. Natl. Acad. Sci USA* **93,** 7032–7035.

Cohen, P. (1997). The search for physiological substrates of MAP and SAP kinases in mammalian cells. *Trends Cell Biol.* **7,** 353–361.

Colas, P., and Dubé, F. (1998). Meiotic maturation in mollusc oocytes. *Semin. Dev. Biol.* **9,** 539–548.

Cross, D. A. E., and Smythe, C. (1998). PD 98059 prevents establishment of the spindle assembly checkpoint and inhibits the G_2-M transition in meiotic, but not mitotic cell cycles in *Xenopus. Exp. Cell Res.* **241,** 12–22.

DeSilva, D. R., Jones, E. A., Favata, M. F., Jaffee, B. D., Magolda, R. L., Trzaskos, J. M., and Scherle, P. A. (1998). Inhibition of mitogen-activated protein kinase kinase blocks T cell proliferation but does not induce or prevent anergy. *J. Immunol.* **160,** 4175–4181.

Dudley, D. T., Pang, L., Decker, S. J., Bridges, A. J., and Saltiel, A. R. (1995). A synthetic inhibitor of the mitogen-activated protein kinase cascade. *Proc. Natl. Acad. Sci. USA* **92,** 7686–7689.

Eckberg, W. R. (1997). MAP and cdc2 kinase activities at germinal vesicle breakdown in *Chaetopterus. Dev. Biol.* **191,** 182–190.

Favata, M. F., Horiuchi, K. Y., Manos, E. J., Daulerio, A. J., Stradley, D. A., Feeser, W. S., Van Dyk, D. E., Pitts, W. J., Earl, R. A., Hobbs, F., Copeland, R. A., Magolda, R. L., Scherle, P. A., and Trzaskos, J. M. (1998). Identification of a novel inhibitor of mitogen-activated protein kinase kinase. *J. Biol. Chem*. **273,** 18623–18632.

Fisher, D., Abrieu, A., Simon, M-N., Keyse, S., Vergé, V., Dorée, M., and Picard, A. (1998). MAP kinase inactivation is required only for G2-M phase transition in early embryogenesis cell cycles of the starfishes *Marthasterias glacialis* and *Astropecten aranciacus. Dev. Biol.* **202,** 1–13.

Furuno, N., Nishizawa, M., Okazaki, K., Tanaka, H., Iwashita, J., Nakajo, N., Ogawa, Y., and Sagata, N. (1994). Suppression of DNA replication via Mos function during meiotic divisions in *Xenopus* oocytes. *EMBO J.* **13,** 2399–2410.

Gavin, A-C., Cavadore, J-C., and Schorderet-Slatkine, S. (1994). Histone H1 kinase activity, germinal vesicle breakdown and M phase entry in mouse oocytes. *J. Cell. Sci.* **107,** 275–283.

Giloh, H., and Sadat, J. W. (1982). Fluorescence microscopy: Reduction in photobleaching of rhodamine and fluorescein protein conjugates by n-propyl gallate. *Science* **217,** 1252–1255.

Gould, M. C. (1967). Echiuroid worms: *Urechis. In* "Methods in Developmental Biology" (F. H. Wilt and N. K. Wessells, Eds.), pp. 277–311. Crowell, New York.

Gould, M. C. (1968). Completion of the first meiotic division after fertilization in *Urechis caupo* eggs despite inhibition of protein synthesis. *J. Cell. Biol.* **38,** 220–224.

Gould, M. C., and Stephano, J. L. (1991). Peptides from sperm acrosomal protein that initiate egg development. *Dev. Biol.* **146,** 509–518.

Gould, M. C., and Stephano, J. L. (1993). Nuclear and cytoplasmic pH increase at fertilization in *Urechis caupo. Dev. Biol.* **159,** 608–617.

Gould, M. C., and Stephano, J. L. (1996). Fertilization and parthenogenesis in *Urechis caupo* (Echiura). *Invert. Reprod. Dev.* **30,** 17–22.

Guadagno, T. M., and Ferrell, J. E., Jr. (1998). Requirement for MAPK activation for normal mitotic progression in *Xenopus* egg extracts. *Science* **282,** 1312–1315.

Gunderson, G. G., and Cook, T. A. (1999). Microtubules and signal transduction. *Curr. Opin. Cell Biol.* **11,** 81–94.

Hirai, S., Nagahama, Y., Kishimoto, T., and Kanatani, H. (1981). Cytoplasmic maturity revealed by the structural changes in incorporated spermatozoon during the course of oocyte maturation. *Dev. Growth Differ.* **23,** 465–478.

Kato, K. H., Washitani-Nemoto, S., Hina, A., and Namoto, S-I. (1990). Ultrastructural studies on the behavior of centrioles during meiosis of starfish oocytes. *Dev. Growth Differ.* **32,** 41–49.

Katsu, Y., Minshall, N., Nagahama, Y., and Standart, N. (1999). Ca^{2+} is required for phosphorylation of clam p82/CPEB *in vitro:* Implications for dual and independent roles of MAP and cdc2 kinases. *Dev. Biol.* **209,** 186–199.

Kuriyama, R., Borisy, G. G., and Masui, Y. (1986). Microtubule cycles in oocytes of the surf clam, *Spisula solidissima:* An immunofluorescence study. *Dev. Biol.* **114,** 151–160.

Laemmli, U. K. (1970). Cleavage of structural proteins during the assembly of the head of bacteriophage T4. *Nature* **227,** 680–685.

Longo, F. J., and Anderson, A. (1970). An ultrastructural analysis of fertilization in the surf clam, *Spisula solidissima.* II. Development of the male pronucleus and the association of the maternally and paternally derived chromosomes. *J. Ultrastruct. Res.* **33,** 515–527.

Luykx, P. (1991). Behavior of egg and sperm centrioles in fertilized eggs of *Urechis caupo. Cytobios* **66,** 7–19.

Miller, J. H., and Epel, D. (1973). Studies of oogenesis in *Urechis caupo*. II. Accumulation during oogenesis of carbohydrate, RNA, microtubule protein, and soluble, mitochondrial, and lysosomal enzymes. *Dev. Biol.* **32,** 331–344.

Miyazaki, S., and Hirai, S. (1979). Fast polyspermy block and activation potential. *Dev. Biol.* **70,** 327–340.

Newby, W. W. (1932). The early embryology of the echiuroid, *Urechis*. *Biol. Bull.* **63,** 387–399.

Oka, M. T., Arai, T., and Hamaguchi, Y. (1990). Heterogeneity of microtubules in dividing sea urchin eggs revealed by immunofluorescence microscopy: Spindle microtubules are composed of tubulin isotypes different from those of astral microtubules. *Cell Motil. Cytoskel.* **16,** 239–250.

Paul, M. (1975). Release of acid and changes in light scattering properties following fertilization of *Urechis caupo*. *Dev. Biol.* **43,** 299–312.

Picard, A., Galas, S., Peaucellier, G., and Doreé, M. (1996). Newly assembled cyclin B-cdc2 kinase is required to suppress DNA replication between meiosis I and meiosis II in starfish oocytes. *EMBO J.* **15,** 3590–3598.

Picard, A., and Peaucellier, G. (1998). Behavior of cyclin B and cyclin B-dependent kinase during starfish oocyte meiosis reinitiation: Evidence for non-identity with MPF. *Biol. Cell* **90,** 487–496.

Roy, L. M., Haccard, O., Izumi, T., Lattes, B. G., Lewellyn, A. L., and Maller, J. L. (1996). Mos proto-oncogene function during oocyte maturation in *Xenopus*. *Oncogene* **12,** 2203–2211.

Sadler, K. C., and Ruderman, J. V. (1998). Components of the signaling pathway linking the 1-methyladenine receptor to MPF activation and maturation in starfish oocytes. *Dev. Biol.* **197,** 25–38.

Sagata, N. (1997). What does Mos do in oocytes and somatic cells? *BioEssays* **19,** 13–21.

Schatten, H., Schatten, G., Mazia, D., Balczon, R., and Simerly, C. (1986). Behavior of centrosomes during fertilization and cell division in mouse oocytes and in sea urchin eggs. *Proc. Natl. Acad. Sci. USA* **83,** 105–109.

Shapiro, P. S., Valsberg, E., Hunt, A. J., Tolwinski, N. S., Whalen, A. M., McIntosh, J. R., and Ahn, N. G. (1998). Activation of the MKK/ERK pathway during somatic cell mitosis: Direct interactions of active ERK with kinetochores and regulation of the mitotic 3F3/2 phosphorylation. *J. Cell Biol.* **142,** 1533–1545.

Shibuya, E. K., Boulton, E. G., Cobb, M. H., and Ruderman, J. V. (1992). Activation of p42 MAP kinase and the release of oocytes from cell cycle arrest. *EMBO J.* **11,** 3963–3975.

Sluder, G., Miller, F. J., Lewis, K., Davison, E. D., and Rieder, C. L. (1989). Centrosome inheritance in starfish zygotes: Selective loss of the maternal centrosome after fertilization. *Dev. Biol.* **131,** 567–579.

Stephano, J. L., and Gould, M. C. (1995). Parthenogenesis in *Urechis caupo* (Echiura). I. Persistence of functional maternal asters following activation without meiosis. *Dev. Biol.* **167,** 104–117.

Stephano, J. L., and Gould, M. C. (1997a). Parthenogenesis in *Urechis caupo* (Echiura). II. Role of intracellular pH in parthenogenesis induction. *Dev. Growth Differ.* **39,** 99–104.

Stephano, J. L., and Gould, M. C. (1997b). The intracellular calcium increase at fertilization in *Urechis caupo* oocytes: Activation without waves. *Dev. Biol.* **191,** 53–68.

Stewart-Savage, J., and Grey, R. D. (1982). The temporal and spatial relationships between cortical contraction, sperm trail formation, and pronuclear migration in fertilized *Xenopus* eggs. *Roux's Arch. Dev. Biol.* **191,** 241–245.

Tachibana, K., Machida, T., Nomura, Y., and Kishimoto, T. (1997). MAP kinase links the fertilization signal transduction pathway to the G_1/S-phase transition in starfish eggs. *EMBO J.* **16,** 4333–4339.

Tyler, A. (1965). The biology and chemistry of fertilization. *Am. Natur.* **97,** 309–334.

Verlhac, M-H., Kubiak, J. Z., Clarke, H. J., and Maro, B. (1994). Microtubule and chromatin behavior follow MAP kinase activity but not MPF activity during meiosis in mouse oocytes. *Development* **120,** 1017–1025.

Walker, J., Dale, M., and Standart, N. (1996). Unmasking mRNA in clam oocytes: Role of phosphorylation of a 3′ UTR masking element-binding protein at fertilization. *Dev. Biol.* **173,** 292–305.

Watanabe, N., Hunt, T., Ikawa, Y., and Sagata, N. (1991). Independent inactivation of MPF and cytostatic factor (Mos) upon fertilization of *Xenopus* eggs. *Nature* **352,** 247–248.

Wilson, E. B. (1928). "The Cell in Development and Heredity," 3rd ed., pp. 394–449. Macmillan, New York.

Wilson, E. B., and Mathews, A. P. (1895). Maturation, fertilization and polarity in the echinoderm egg. *J. Morphol.* **10,** 319.

Wu, X., and Palazzo, R. E. (1999). Differential regulation of maternal vs. paternal centrosomes. *Proc. Natl. Acad. Sci. USA* **96,** 1397–1402.

Zecevic, M., Catling, A. D., Eblen, S. T., Renzi, L., Hittle, J. C., Yen, T. J., Gorbsky, G. J., and Weber, M. J. (1998). Active MAP kinase in mitosis: Localization at kinetochores and association with the motor protein CENP-E. *J. Cell. Biol.* **142,** 1547–1558.

Zhao, X., Singh, B., and Batten, B. E. (1991). The role of c-*mos* proto-oncoprotein in mammalian meiotic maturation. *Oncogene* **6,** 43–49.

Zimmerman, W., Sparks, C. A., and Dixsey, S. J. (1999). Amorphous no longer: The centrosome comes into focus. *Curr. Opin. Cell Biol.* **11,** 122–128.

Received for publication May 27, 1999
Revised August 23, 1999
Accepted August 24, 1999